Cancer Science
Japanese Cancer Association JCA
Open Access

ECT2 amplification and overexpression as a new prognostic biomarker for early-stage lung adenocarcinoma

Yoshihiko Murata,[1] Yuko Minami,[2]* Reika Iwakawa,[3] Jun Yokota,[3] Shingo Usui,[1] Koji Tsuta,[4] Kouya Shiraishi,[3] Shingo Sakashita,[2] Kaishi Satomi,[2] Tatsuo Iijima[5] and Masayuki Noguchi[2]

[1]Department of Pathology, Graduate School of Comprehensive Human Sciences; [2]Department of Pathology, Faculty of Medicine, University of Tsukuba, Ibaraki; [3]Division of Genome Biology; [4]Pathology Division, National Cancer Center Research Institute, Tokyo; [5]Department of Pathology, Ibaraki Prefectural Central Hospital, Ibaraki, Japan

Key words

3q26 Region, array-comparative genomic hybridization, early-stage lung adenocarcinoma, *ECT2*, prognostic biomarker

Correspondence

Yuko Minami, Department of Pathology, Faculty of Medicine, University of Tsukuba, 1-1-1 Tennodai, Tsukuba-shi, Ibaraki 3058575, Japan.
Tel: +81-29-853-3150; Fax: +81-29-853-3150;
E-mail: minami-y@md.tsukuba.ac.jp

Funding Information

Ministry of Education, Culture, Sports, Science and Technology of Japan (23501294). Ministry of Health, Labor and Welfare of Japan.

Received October 30, 2013; Revised January 21, 2014; Accepted January 26, 2014

Cancer Sci **105** (2014) 490–497

doi: 10.1111/cas.12363

Genetic abnormality in early-stage lung adenocarcinoma was examined to search for new prognostic biomarkers. Six *in situ* lung adenocarcinomas and nine small but invasive adenocarcinomas were examined by array-comparative genomic hybridization, and candidate genes of interest were screened. To examine gene abnormalities, 83 cases of various types of lung carcinoma were examined by quantitative real-time genomic PCR and immunohistochemistry. The results were then verified using another set of early-stage adenocarcinomas. Array-comparative genomic hybridization indicated frequent amplification at chromosome 3q26. Of the seven genes located in this region, we focused on the epithelial cell transforming sequence 2 (*ECT2*) oncogene, as *ECT2* amplification was detected only in invasive adenocarcinoma, and not in *in situ* carcinoma. Quantitative PCR and immunohistochemistry analyses also detected overexpression of ECT2 in invasive adenocarcinoma, and this was correlated with both the Ki-67 labeling index and mitotic index. In addition, it was associated with disease-free survival and overall survival of patients with lung adenocarcinoma. These results were verified using another set of early-stage adenocarcinomas resected at another hospital. Abnormality of the *ECT2* gene occurs at a relatively early stage of lung adenocarcinogenesis and would be applicable as a new biomarker for prognostication of patients with lung adenocarcinoma.

Lung adenocarcinoma is the leading cause of cancer death in Japan and other developed countries such as the USA and UK, and in western Europe. Various gene abnormalities, including mutations of *KRAS*, *p53*, and *EGFR*, amplifications of *PIK3CA*, *BRAF*, and *HER2*, and translocations of *ALK*, *ROS*, and *RET* have been reported in lung adenocarcinoma.[1–9] Such gene abnormalities are usually detected at the advanced stage and, apart from *EGFR* mutation, their frequency in early-stage adenocarcinoma is very low. However, few studies have detected specific copy number aberrations in lung adenocarcinoma, except for *EGFR*, *c-myc*, and *Met*.[10–12]

Among the various methods for analyzing genome abnormality, array-comparative genomic hybridization (CGH) was developed to detect increases in gene copy number in cell lines harboring amplification of oncogenes.[13] Array-CGH is a useful procedure in cancer research, as it can detect low copy-number gains and losses by use of chromosome-specific DNA libraries.[14,15] Inazawa *et al.*[16] originally developed the array-CGH method for identifying specific chromosomal aberrations in solid tumors that might be associated with carcinogenesis.

Recently, the new WHO classification of adenocarcinoma was proposed by the International Association for the Study of Lung Cancer.[17] In this system, lung adenocarcinoma was classified according to the time-course of malignant progression as adenocarcinoma *in situ* (AIS), minimally invasive adenocarcinoma, or invasive adenocarinoma. This new concept was based on the clinical outcome of various histological types of lung adenocarcinoma. In 1995, Noguchi *et al.*[18] suggested a prototype histological classification of small-sized adenocarcinomas that comprised six subtypes, Types A–F. Type A and B tumors were classified as early-stage adenocarcinomas, whereas Types C–F were classified as invasive adenocarcinomas. Type A and B tumors show an extremely favorable prognosis (5-year survival rate, 100%). Types D–F tumors are early but definitely invasive (5-year survival rate, 50%). Type C tumors include those showing both favorable and unfavorable outcomes (5-year survival rate, 75%).

In the present study, we focused on early lung adenocarcinoma and examined differences in gene abnormalities between AIS (Types A and B) and early-invasive adenocarcinomas (Types D and E) using the array-CGH method. Finally, we detected epithelial cell transforming sequence 2 oncogene (*ECT2*) abnormality as a new prognostic biomarker of lung adenocarcinoma and characterized its clinicopathological features.

Materials and Methods

Patients. Among cases of lung carcinoma resected at Tsukuba University Hospital (Ibaraki, Japan) between 1996 and 2012, 140 adenocarcinomas were fixed with both 10% formalin and 100% methanol. We selected 83 cases for analysis in this study, and these included 32 small-sized adenocarcinomas. Among these cases, 15 fresh small-sized adenocarcinomas including six AIS (Type A or B adenocarcinoma) and nine early-invasive adenocarcinomas (Type D or E adenocarcinoma) were subjected to array-CGH analysis. All 83 cases were examined by quantitative real-time genomic PCR (qPCR) and 66 cases of invasive adenocarcinoma by immunohistochemistry (IHC). Pathological stage was evaluated according to the UICC TNM Classification of Malignant Tumors, 7th edition.[19]

Array-CGH. Six AIS (Type A or B adenocarcinoma), nine early-invasive adenocarcinomas (Type D or E adenocarcinoma), and normal lung tissues from each case were used for array-CGH. The tumor area was microdissected using an LM-200 laser-capture microdissection system (Arcturus Engineering, Mountain View, CA, USA). Microdissected and extracted genomic DNAs were amplified using a whole-genome amplification kit. We then examined copy-number aberrations using Cancer Array-800, containing 800 bacterial artificial chromosome (BAC) clones with 786 known cancer-related genes (http://www.cghtmd.jp/cghdatabase/index.html).[16] DNAs that differed between normal lung and tumor tissue and BAC clones were hybridized, then the hybridized slides were scanned with a GenePix Pro 5.0 (Axon Instruments, Foster City, CA, USA). Fluorescence ratios were normalized so that the mean value of the signal intensities obtained by the array was 1.00. Thresholds of signal ratios corresponding to chromosomal losses, gains, amplifications, and homozygous deletions were determined by the Gaussian mixture method using ACUE2 analytical software (Mitsui Knowledge Industry, Tokyo, Japan).[20]

Quantitative real-time genomic PCR. After comparing the gene copy number abnormalities, several candidate gene alterations were evaluated using a large number of samples. One hundred and one methanol-fixed tumors, including 15 AIS (Type A or B tumors) and 17 early-invasive adenocarcinomas (Type D or E tumors) were examined by qPCR. All materials were fixed with methanol and embedded in paraffin. Genomic DNA was extracted from 10-μm-thick sections by digestion with proteinase K, followed by use of a QIAamp DNA Mini Kit (Qiagen, Düsseldorf, Germany). Oligonucleotide primers for *ECT2*, eukaryotic translation initiation factor 5A2 (*EIF5A2*), tumor necrosis factor (ligand) superfamily, member 10 (*TNFSF10*), ecotropic viral integration site 1 (*EVI1*), SKI-like oncogene (*SKIL*), and mucin 4 (*MUC4*) were designed using Primer3 (http://primer3.sourceforge.net/), and phosphatidylinositol-4,5-bisphosphate 3-kinase, catalytic subunit alpha (*PIK3CA*) primer sets were prepared according to Soh *et al.*[21] *GAPDH* was used as an internal control gene for normalization. Quantitative PCR analysis was carried out using SYBR Premix Ex Taq (Perfect Real Time; Takara Bio, Tokyo, Japan). The PCR reactions were carried out using an ABI 7300 Sequence Detection System (Applied Biosystems, Foster City, CA, USA) at 95°C for 30 s followed by 40 cycles of 95°C for 5 s and 60°C for 31 s. A ratio (tumor/normal) of ≥1.5 was defined as representing gene amplification.

Immunohistochemical staining. Immunohistochemistry was carried out on the same 101 tumors using qPCR analysis. All tumors were fixed in 10% formalin and embedded in paraffin. The deparaffinized and dehydrated 3-μm-thick sections were autoclaved in 10 mM tris-HCl (pH 8), 1 mM EDTA (1 × Tris-EDTA; TE buffer) at 105°C for 15 min for antigen retrieval, then incubated with polyclonal anti-ECT2 antibody diluted 1:200 (catalog no. 07-1364; Millipore, Billerica, MA, USA), polyclonal anti-EIF5A2 antibody diluted 1:100 (catalog no. HPA029090, Sigma, St. Louis, MO, USA), monoclonal anti-PIK3CA antibody diluted 1:100 (catalog no. 4249S, C73F8; Cell Signaling Technology, Danvers, MA, USA), and polyclonal anti-TNFSF10 antibody diluted 1:50 (catalog no. sc-6079; Santa Cruz Biotechnology, Dallas, TX, USA) for 30 min at room temperature. In order to examine cell proliferative activity, we also stained Ki-67 using the MIB-1 antibody diluted 1:100 (Dako, Glostrup, Denmark). Sections were autoclaved in 10 mM citrate buffer (pH 6.0) at 121°C for 10 min for antigen retrieval, then incubated with the above antibody for 30 min at room temperature. Subsequently, the sections of ECT2, EIF5A2, PIK3CA, and Ki-67 were incubated with EnVision+ Dual Link System–HRP Polymer Reagent (Dako, Carpinteria, CA, USA) for 30 min at room temperature, and the sections of TNFSF10 were incubated with Histofine Simple Stain MAX PO(G) (Nichirei Bioscience, Tokyo, Japan) for 30 min at room temperature. Immunoreactivity was detected with a diaminobenzidine substrate kit (Dako Japan, Tokyo, Japan), and the sections were counterstained with hematoxylin.

Evaluation of IHC. For EIF5A2, PIK3CA, and TNFSF10 staining, the sections were evaluated for the percentage of tumor cells showing positive nuclear membranous staining for EIF5A2 or positive cytoplasmic staining (0–100%) for PIK3CA and TNFSF10, and the intensity of positive staining was evaluated on a scale from 0 to 2+ (0, complete absence of staining; 1+, weak; 2+, staining clearly more intense than that of normal bronchial epithelium). Negative controls were mature lymphocytes for EIF5A2, bronchial epithelial cells for PIK3CA, and alveolar epithelial cells for TNFSF10. The percentage and the intensity of immunoreactivity were multiplied to give a scoring index ranging from 0 to 200.[22–24]

For ECT2 staining, 1000 tumor cells were evaluated for the most intense nuclear staining (hot spot) according to the method of Iyoda *et al.*[25] with minor modifications. Alveolar epithelial cells were used as a negative control.[26] The ECT2 IHC score was determined as the count of stained nuclei in 1000 tumor cells.

Ki-67 staining in tumor cells was evaluated as the percentage of positive tumor cells showing the most intense nuclear staining (hot spot).

Fluorescence *in situ* hybridization. Formalin-fixed, paraffin-embedded serial sections 5-μm thick were subjected to dual-color FISH using an ECT2/CEN3q probe cocktail (GSP Lab., Kanagawa, Japan). After deparaffinization and dehydration, all slides were incubated in pretreatment solution for 30 min at 98°C, and immersed in protease solution for 10 min at 37°C. After co-denaturation of the probe, DNA in the tissue sections was hybridized by incubation at 75°C for 5 min followed by incubation at 37°C for 72 h. After hybridization, the slides were counterstained with DAPI. Using a fluorescence microscope with single interference filter sets for green (FITC), red (TexRed), and blue (DAPI), FISH signals were enumerated in non-overlapping tumor cell nuclei.

Validation of results. *ECT2* amplification and overexpression and its relationship with patient outcome were validated using another set of small-sized adenocarcinomas that had been resected at the National Cancer Center Hospital

(Tokyo, Japan). Sixty-four small-sized adenocarcinomas including 14 AIS (Type A or B tumors) and 50 early-invasive adenocarcinomas (Type C or D tumors) were examined by GeneChip Human Mapping 10K SNP array (Affymetrix, Santa Clara, CA, USA), and 144 early-stage (Stage I) adenocarcinomas were analyzed by Affymetrix U133 Plus 2.0 array (Affymetrix) as described previously.[12,27]

Statistical analysis. For array-CGH, hierarchical clustering analysis was carried out using the Impressionist (Gene Data, Basel, Switzerland) and GeneMaths (Applied Maths, Saint-Martens-Latem, Belgium) software packages. Statistical analysis related to detection and standardization of gene correlations with the Noguchi classification was carried out using Welch's *t*-test and *Z*-test. False positivity rates were estimated using the family-wise error rate and false discovery rate by *t*-test and *Z*-test. Detection of gene variance and also amplification and deletion of chromosomal location were analyzed using Fisher's combined probability test.

Analysis of the correlation between the results of qPCR and IHC was carried out using Pearson's correlation test. Survival curves were generated using the Kaplan–Meier method, and the running log–rank test was used to assess the statistical significance of differences between the groups. Prognostic variables identified by univariate analysis were analyzed using the χ^2-test. Statistical significance was defined as $P < 0.05$. Statistical analyses were carried out using the SPSS 11.5J software package (SPSS Inc., Chicago, IL, USA).

For the National Cancer Center data, Fisher's exact test was used to assess the association of *ECT2* amplification with Noguchi's classification. Relapse-free survival (RFS) and overall survival (OS) of patients with ECT2 expression was compared using Kaplan–Meier curves and the log–rank test. The Cox proportional hazard model was used to compute univariate and multivariate hazard ratios and the 95% confidence intervals. Statistical analyses were carried out using JMP software (version 5.1; SAS Institute, Cary, NC, USA).

Results

Cancer Array-800. Using array-CGH, genetic aberration was compared between six AIS (Type A or B adenocarcinomas) and nine early-invasive adenocarcinomas (Type D or E adenocarcinomas). The pathological stage of the six AIS was pStage IA and those of the nine early-invasive adenocarcinomas included four pStage IA, three pStage IB, one pStage IIA, and one pStage IIIA. Although gene alterations were detected at various sites on chromosomes in both AIS (Types A or B) and early-invasive adenocarcinoma (Types D and E), the total number observed was significantly higher in Type D or E than in Type A or B ($P < 0.01$; data not shown). Among these gene alterations, gene amplifications in early-invasive adenocarcinomas were significantly more frequent at 3q (including 27 genes) than in AIS ($P < 0.01$; Fig. S1). According to the BAC map of Cancer Array-800, seven genes – *ECT2*, *EIF5A2*, *EVI1*, *PIK3CA*, *TNFSF10*, *SKIL*, and *TERC* – were located at 3q26. As these genes have also been reported to have an association with cancer malignancy, we targeted them and confirmed the results by qPCR using a large number of cases.

Quantitative real-time genomic PCR. The targeted genes at 3q26, *ECT2*, *EIF5A2*, *EVI1*, *PIK3CA*, *TNFSF10*, and *SKIL*, except for *TERC*, were examined by qPCR assay. *TERC* was excluded because it is constituted wholly by RNA, and consequently it was difficult to devise primers including the intron region. Instead, *MUC4* at 3q29 was additionally examined, as it showed a significantly higher frequency of amplification in early-invasive adenocarcinoma than in AIS.

The seven selected gene amplifications were examined using 15 AIS (Type A or B) and 17 early-invasive adenocarcinomas (Type D or E) by qPCR (Fig. 1a). All seven genes showed amplification in early-invasive adenocarcinomas, confirming the results of Cancer Array-800. However, several cases of AIS showed amplification of *EVI1*, *SKIL*, and *MUC4*. In contrast, *ECT2*, *EIF5A2*, *PIK3CA*, and *TNFSF10* showed no amplification in AIS. Additionally, 51 advanced lung adenocarcinomas, giving a total of 83 adenocarcinomas, were also examined by qPCR. Altogether, seven cases (8%) were amplified at *ECT2*, seven (8%) at *EIF5A2*, nine (11%) at *PIK3CA*, and eight (10%) at *TNFSF10* (Fig. 1b).

On the basis of these results, we focused on the *ECT2*, *EIF5A2*, *PIK3CA*, and *TNFSF10* genes and examined the clinical significance of these gene alterations in lung adenocarcinoma.

Correlation between qPCR and IHC. Using the 83 cases, IHC for *ECT2*, *EIF5A2*, *PIK3CA*, and *TNFSF10* was carried out. Although faint staining was detected in the cytoplasm of the tumor cells, nuclei were mainly stained by antibody against *ECT2* (Fig. 2a). For other genes, the cytoplasm or nuclear membrane was stained. The results showed a slight correlation with those of qPCR. The correlation coefficients were: $r = 0.36$ for *ECT2*; $r = 0.07$ for *EIF5A2*; $r = 0.13$ for *PIK3CA*; and $r = 0.14$ for *TNFSF10*. Of these four genes, *ECT2* was correlated most closely with the qPCR value.

In order to confirm the relationship between *ECT2* amplification and ECT2 overexpression, FISH analysis was carried out for three cases that showed high amplification by qPCR analysis (Fig. 2b). The signals were enumerated in 100 non-overlapping tumor cell nuclei. As shown in the figure, we confirmed the amplification signal in the three tumors.

Correlation between *ECT2* and Ki-67, and its clinicopatholgical significance. Immunohistochemical analysis of *ECT2* and Ki-67 showed similar staining patterns in lung adenocarcinoma, and ECT2 expression was correlated with the Ki-67 labeling index ($r = 0.76$) and mitotic index ($r = 0.87$).

Next, we examined the relationship between ECT2 overexpression and patient outcome. Based on the IHC results for all 66 invasive adenocarcinomas, the tumors were divided into a high ECT2 score group (>140) and a low ECT2 score group (≤140) by log–rank test. In patients with invasive adenocarcinoma, a high ECT2 score was significantly associated with poorer survival (OS, $P = 0.0096$; disease-free survival, $P = 0.019$; Fig. S2). We then carried out univariate analyses using different covariates, including smoking and tumor size (T factor), lymph node metastasis (N factor), distant metastasis (M factor), pathological stage, pleural invasion, vascular invasion, lymphatic permeation, and histological subtype. N factor ($P = 0.003$), pathological stage ($P = 0.022$), vascular invasion ($P = 0.004$), histological subtype ($P = 0.0001$), and smoking ($P = 0.038$) were significantly correlated with high ECT2 expression (Table 1).

Validation of single-institution analysis. In order to confirm the present results, we used the database of the National Cancer Center Hospital. From the GeneChip Human Mapping 10K SNP array (Affymetrix) database, we examined 64 small-sized adenocarcinomas including 14 AIS (Types A and B) and 50 early-invasive adenocarcinomas (Types C and D). Thirteen

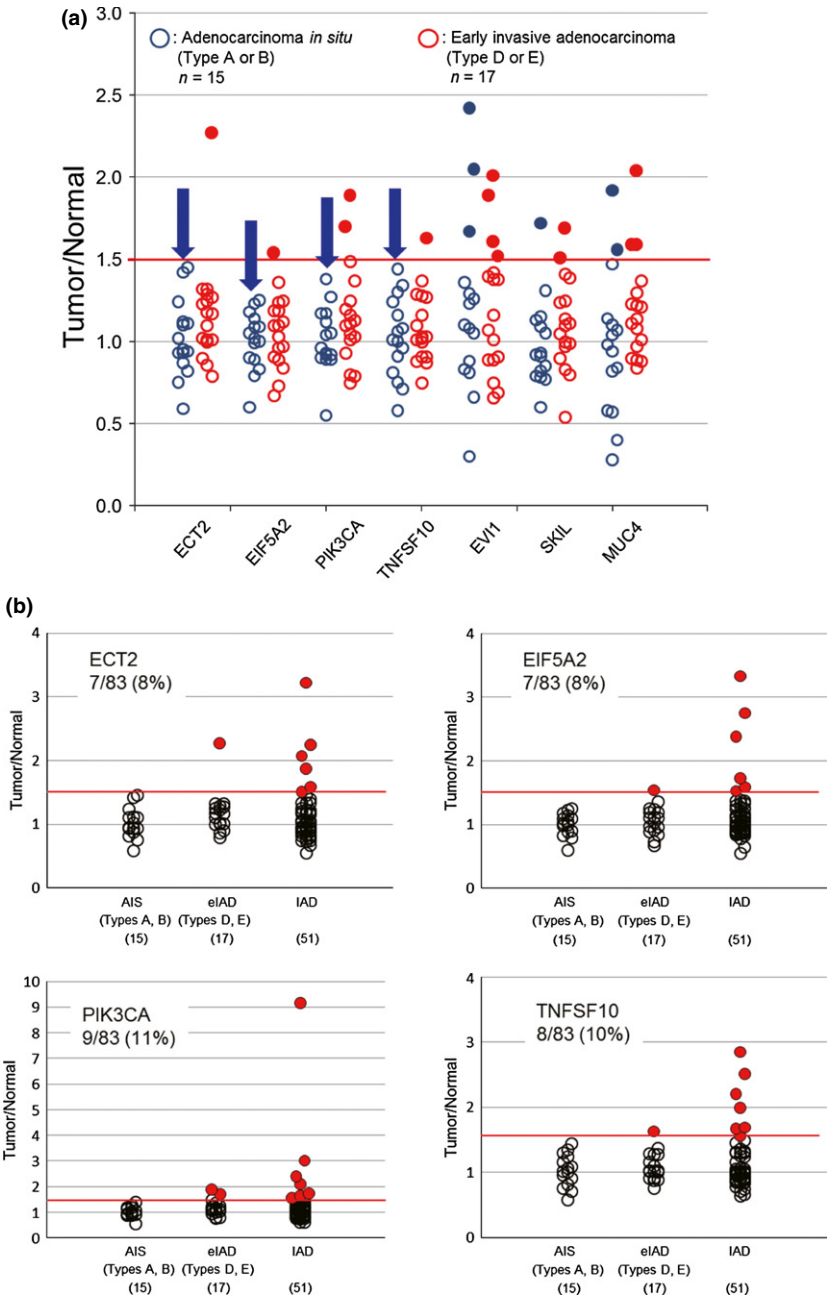

Fig. 1. (a) Amplification of seven selected genes was examined using 15 adenocarcinomas *in situ* (AIS; Type A or B; blue dot) and 17 early-invasive adenocarcinomas (eIAD; Type D or E; red dot) by quantitative real-time genomic PCR. The *ECT2*, *EIF5A2*, *PIK3CA*, and *TNFSF10* genes showed no amplification in AIS (blue arrows). (b) Quantitative real-time genomic PCR was carried out for *ECT2*, *EIF5A2*, *PIK3CA*, and *TNFSF10* in 83 lung adenocarcinomas. Values in parentheses indicate the number of cases tested for each type of carcinoma. Seven cases (8%) showed amplification of *ECT2*, seven (8%) for *EIF5A2*, nine (11%) for *PIK3CA*, and eight (10%) for *TNFSF10*. IAD, invasive adenocarcinoma.

cases of early-invasive adenocarcinoma (26%) showed amplification at *ECT2*, but none of the AIS did so (Table 2, Fig. S3).

From the cDNA microarray data, 144 early-stage (pStage I) adenocarcinomas were divided into two groups showing high (n = 22) and low (n = 122) expression of ECT2. As shown in Figure 3, the ECT2 high group showed a significantly poorer outcome in terms of both OS rate and RFS rate. Moreover, multivariate analysis showed that ECT2 overexpression was an independent prognostic factor, similar to vascular invasion (Table 3).

Discussion

Comparative genomic hybridization was developed as a molecular cytogenetic technique to compensate for the difficulties presented by conventional cytogenetics and FISH analysis. Array-based CGH uses a cDNA microarray that includes well-defined genomic clones (BACs, PACs, or cosmids). These clones contain sequence information directly connected with the genomic database, and researchers can easily note particular biological aspects of genes that lie within regions involved in copy-number aberrations. In this study, we used Cancer Array-800 and compared copy-number aberrations between lung AIS (Noguchi Type A or B) and early-invasive adenocarcinoma of the lung (Noguchi Type D or E) to find early genetic alterations in the course of malignant progression of lung adenocarcinoma. It is very interesting that a specific region, 3q, showed significant amplification in early-invasive adenocarcinomas, unlike AIS. Amplification at 3q has been reported in various cancers including cervical cancer, liver cancer, melanoma, and squamous cell lung carcinoma.[28–31] In the present study, we found 3q amplification in approximately

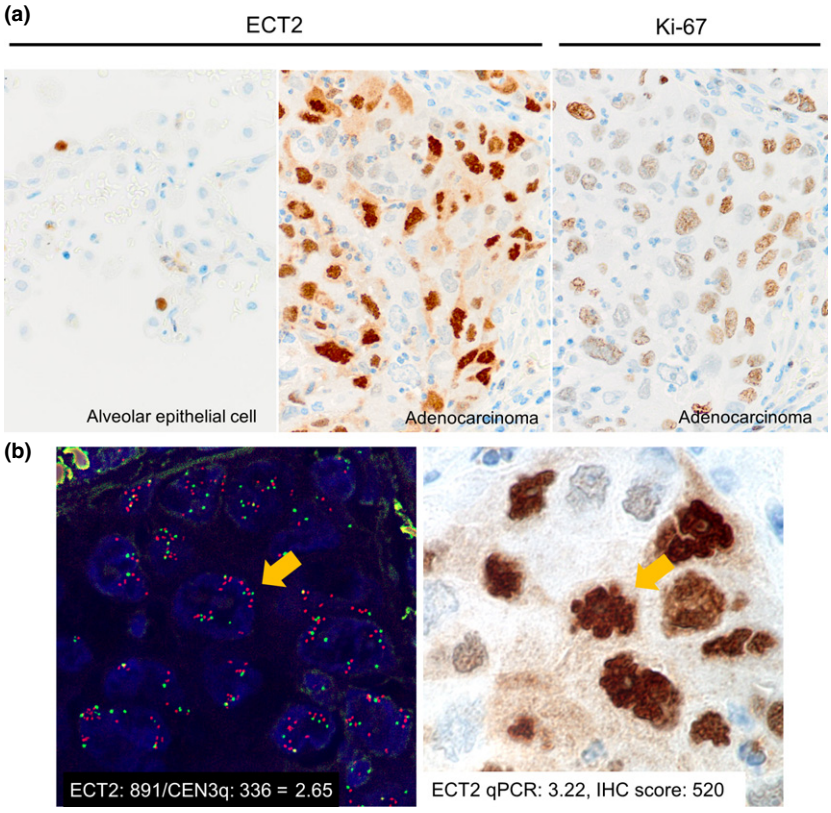

Fig. 2. (a) Immunohistochemical (IHC) staining pattern of ECT2 and Ki-67. The same nuclei were stained by antibody against ECT2 and Ki-67. ECT2 in tumor cells was also stained weakly in the cytoplasm. Alveolar epithelial cells were used as a negative control. (b) FISH (left) and IHC images for one of the tumors showing high *ECT2* amplification. Yellow arrows indicate the same nucleus. Red signal shows the *ECT2* gene. Green signal shows chromosome 3 enumeration. IHC score, the count of stained nuclei in 1000 tumor cells; qPCR, quantitative real-time genomic PCR.

Table 1. Univariate analysis of invasive lung adenocarcinomas (n = 66) based on ECT2 immunohistochemistry scores

	Low (n = 41)	High (n = 25)	P-value
T (1a/1b/2a/2b/3/4)	0/13/19/1/7/1	0/3/12/1/9/0	0.2400
N (0/1/2)	33/3/5	10/7/8	0.0030*
M (0/1)	1 (2.4%)	1 (4.0%)	0.7200
pStage (IA/IB/IIA/IIB/IIIA/IIIB/IV)	12/17/2/3/6/0/1	1/6/4/3/10/0/1	0.0220*
pl (0/1/2/3)	28/7/3/3	12/7/2/4	0.3900
V	16 (39.0%)	19 (76.0%)	0.0040*
Ly	23 (56.1%)	18 (72.0%)	0.2000
Subtype (lepidic/solid/acinar/papillary)	21/1/10/9	3/11/8/3	0.0001*
Smoking history (never/former)	19/22	5/20	0.0380*

Immunohistochemistry score was determined as the count of stained nuclei in 1000 tumor cells. High score, >140; low score, ≤140, by log–rank test. *P < 0.0500.

Table 2. Amplification (amp.) of *ECT2* in early lung adenocarcinoma was verified using GeneChip Human Mapping 10K-SNP array

Histological classification	ECT2 amp. (+)	ECT2 amp. (–)	Total
Adenocarcinoma *in situ* (Types A, B)	0*	14	14
Early-invasive adenocarcinoma (Types C, D)	13	37	50
Total	13	51	64

*P = 0.025, Fisher's exact test.

10% of lung adenocarcinomas. Chromosome 3q26 is also a region that is frequently amplified at the early stage of pulmonary adenocarcinogenesis.

Chromosome 3q contains various genes including those reportedly associated with cancer biology. In the 3q26 region, particularly, several genetic abnormalities were found in lung adenocarcinoma. The *PIK3CA*,[32] *EVI1*,[33] *EIF5A2*,[34] *SKIL*,[35] *TNFSF10*,[36] and *ECT2*[37] genes have already been reported to have some association with lung adenocarcinoma. Among them, we confirmed early-stage amplification and overexpression of ECT2 by qPCR and IHC. The *ECT2* gene is located at 3q26.1–q26.2 and encodes a protein that is a guanine nucleotide exchange factor and transforming protein related to Rho-specific exchange factors and cell cycle regulators. The expression of ECT2 increases with the onset of DNA synthesis and remains elevated during the G_2 and M phases.[26,38–40] In the present study, *ECT2* amplification was detected in 6% of early-invasive adenocarcinomas (1/17 cases; Noguchi Types D or E) treated at Tsukuba University Hospital, whereas it was detected in 26% of early-invasive adenocarcinomas (13/50 cases; Noguchi Types C or D) treated at the National Cancer Center Hospital. This discrepancy may be partly associated with differences in the histological subtypes (Types D or E versus Types C or D) examined at the two hospitals. Histologically, type E adenocarcinoma is diagnosed as acinar (tubular) adenocarcinoma, which is classified into non-terminal respiratory unit-type adenocarcinoma.[41] However, most cases of Types A–D are classified as terminal respiratory unit-type adenocarcinoma. Cases in the latter group are positive for TTF-1 expression and show a peripheral airway cell lineage, whereas cases in the former group include the HNF4a-positive phenotype.[42]

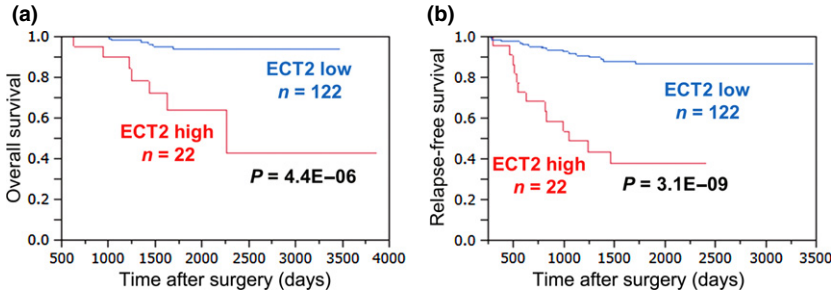

Fig. 3. Kaplan–Meier curves analyzed using the log–rank test showing the overall survival (a) and relapse-free survival (b) of 144 patients with stage I adenocarcinoma.

Table 3. Multivariate analysis of lung adenocarcinoma using cDNA microarray, with *ECT2* overexpression as an independent prognostic factor

Variable	Univariate						Multivariate					
	OS			RFS			OS			RFS		
	HR	95% CI	*P*-value	HR	95% CI	*P*-value	HR	95% CI	*P*-value	HR	95% CI	*P*-value
Age, years (≥60 *vs* <60)	1.14	0.38–3.53	0.8200	1.14	0.65–3.01	0.4200						
Gender (male versus female)	1.22	0.39–3.68	0.7200	1.02	0.47–2.14	0.9600						
Smoking history (+ versus −)	1.73	0.57–5.38	0.3200	1.13	0.53–2.38	0.7500						
Tumor size (>3 cm *vs* ≤3 cm)	1.56	0.42–4.79	0.4700	2.18	0.96–4.65	0.0600						
Lymphatic permeation (+, ± versus −)	4.72	1.54–17.44	0.0064*	4.25	2.00–9.58	0.0002*	1.00	0.24–4.70	>0.9900	1.41	0.58–3.62	0.4600
Vascular invasion (+ versus −)	9.87	3.01–44.06	<0.0001*	6.48	3.00–15.09	<0.0001*	5.06	1.13–28.15	0.0330*	3.76	1.42–10.30	0.0076*
Pleural invasion (1, 2 *vs* 0)	1.33	0.20–4.98	0.7200	1.76	0.59–4.26	0.2800						
pStage_ver.7 (IB versus IA)	2.32	0.75–6.98	0.1400	3.04	1.44–6.44	0.0041*				2.95	0.62–13.39	0.1700
EGFR mutation (+ versus −)	0.44	0.14–1.33	0.1400	0.52	0.25–1.11	0.0910						
K-ras mutation (+ versus −)	1.95E-06	1.67–1.67	0.1200	0.86	0.14–2.88	0.8300						
ECT2 expression (high versus low) 234992_x_at	8.45	2.80–26.32	0.0003*	7.04	3.28–14.92	<0.0001*	11.67	2.57–60.07	0.0016*	6.54	2.54–16.83	<0.0001*

*$P < 0.0500$. CI, confidence interval; HR, hazard ratio; OS, overall survival; RFS, relapse-free survival.

It is very interesting that *ECT2* amplification is associated with overexpression of ECT2 (Fig. 2b). The correlation between copy-number alterations and gene expression has not been generally proven. Using FISH and IHC, we were able to demonstrate several cases showing *ECT2* amplification and overexpression of ECT2. Overexpression of ECT2 in lung adenocarcinoma was thought to correlate with gene amplification. As the two figures indicate, cases examined in the two hospitals showed a significant difference of OS and disease-free survival or RFS between those with high and low ECT2 expression. Moreover, in the analysis of cases treated at the National Cancer Center Hospital, ECT2 overexpression was an independent prognostic factor together with lymphatic permeation, vascular invasion, and pathological stage. As ECT2 expression is reported to increase with onset of DNA synthesis and remains elevated during the G_2 and M phases, it is reasonable that ECT2 overexpression was correlated with Ki-67 expression and the mitotic index. The Ki-67 IHC score and mitotic index are very useful prognostic markers used as routine biomarkers, and should be examined in general hospitals. The biological significance of a high Ki-67 index may lie in abnormal expression of ECT2. These results indicate that overexpression of ECT2 is a very simple but useful biomarker that can predict patient outcome. Normal ECT2 is localized in the nucleus but oncogenic ECT2 has been reported to move to the cytoplasm and activate a small molecule, GTPase (Rho A, Rac 1, and Cdc42). However, oncogenic ECT2 also associates with PKCι to form the PKCι-Par6-ECT2 complex, which is

thought to drive transformed growth through activation of the Rac1-Pak-Mek1, 2-Erk1,2 signaling axis.[43] In this study, we detected ECT2 not only in the nucleus but also in the cytoplasm of the tumor cells (Fig. 2). Although the staining intensity of ECT2 in the cytoplasm was very faint and we did not include the staining intensity of ECT2, it might be more important for estimating the malignancy of tumor cells than nuclear staining.

As *EGFR*, *MET*, *HER2*, and *KRAS* are known to activate PKCι, these oncogenes are candidate upstream oncogenes of ECT2. Further studies will be required to clarify the relationship between ECT2 overexpression and upstream oncogene aberrations. It is very important to clarify the molecular mechanism responsible for abnormal expression of ECT2 in order to gain further understanding of the early progression of lung adenocarcinoma and design drugs for ECT2-targeted therapy.

Acknowledgments

This work was supported in part by Grants-in-Aid for Scientific Research from the Ministry of Education, Culture, Sports, Science and Technology of Japan (no. 23501294) to Y.M. and the Ministry of Health, Labor and Welfare of Japan to M.N.

Disclosure Statement

The authors have no conflict of interest.

References

1 Kosaka T, Yatabe Y, Endoh H, Kuwano H, Takahashi T, Mitsudomi T. Mutations of the epidermal growth factor receptor gene in lung cancer: biological and clinical implications. *Cancer Res* 2004; **64**: 8919–23.
2 Slebos RJ, Kibbelaar RE, Dalesio O *et al.* K-ras oncogene activation as a prognostic marker in adenocarcinoma of the lung. *N Engl J Med* 1990; **323**: 561–5.
3 Greenblatt MS, Bennett WP, Hollstein M, Harris CC. Mutations in the p53 tumor suppressor gene: clues to cancer etiology and molecular pathogenesis. *Cancer Res* 1994; **54**: 4855–78.
4 Brose MS, Volpe P, Feldman M *et al.* BRAF and RAS mutations in human lung cancer and melanoma. *Cancer Res* 2002; **62**: 6997–7000.
5 Arcila ME, Chaft JE, Nafa K *et al.* Prevalence, clinicopathologic associations, and molecular spectrum of ERBB2 (HER2) tyrosine kinase mutations in lung adenocarcinomas. *Clin Cancer Res* 2012; **18**: 4910–8.
6 Kawano O, Sasaki H, Okuda K *et al.* PIK3CA gene amplification in Japanese non-small cell lung cancer. *Lung Cancer* 2007; **58**: 159–60.
7 Imielinski M, Berger AH, Hammerman PS *et al.* Mapping the hallmarks of lung adenocarcinoma with massively parallel sequencing. *Cell* 2012; **150**: 1107–20.
8 Soda M, Choi YL, Enomoto M *et al.* Identification of the transforming EML4-ALK fusion gene in non-small-cell lung cancer. *Nature* 2007; **448**: 561–6.
9 Takeuchi K, Soda M, Togashi Y *et al.* RET, ROS1 and ALK fusions in lung cancer. *Nat Med* 2012; **18**: 378–81.
10 Hirsch FR, Varella-Garcia M, Bunn PA Jr *et al.* Epidermal growth factor receptor in non-small-cell lung carcinomas: correlation between gene copy number and protein expression and impact on prognosis. *J Clin Oncol* 2003; **21**: 3798–807.
11 Cappuzzo F, Marchetti A, Skokan M *et al.* Increased MET gene copy number negatively affects survival of surgically resected non-small-cell lung cancer patients. *J Clin Oncol* 2009; **27**: 1667–74.
12 Iwakawa R, Kohno T, Kato M *et al.* MYC amplification as a prognostic marker of early-stage lung adenocarcinoma identified by whole genome copy number analysis. *Clin Cancer Res* 2011; **17**: 1481–9.
13 Kallioniemi A, Kallioniemi OP, Sudar D *et al.* Comparative genomic hybridization for molecular cytogenetic analysis of solid tumors. *Science* 1992; **258**: 818–21.
14 Pinkel D, Segraves R, Sudar D *et al.* High resolution analysis of DNA copy number variation using comparative genomic hybridization to microarrays. *Nat Genet* 1998; **20**: 207–11.
15 Solinas-Toldo S, Lampel S, Stilgenbauer S *et al.* Matrix-based comparative genomic hybridization: biochips to screen for genomic imbalances. *Genes Chromosom Cancer* 1997; **20**: 399–407.
16 Inazawa J, Inoue J, Imoto I. Comparative genomic hybridization (CGH)-arrays pave the way for identification of novel cancer-related genes. *Cancer Sci* 2004; **95**: 559–63.
17 Travis WD, Brambilla E, Noguchi M *et al.* International Association for the Study of Lung Cancer/American Thoracic Society/European Respiratory Society international multidisciplinary classification of lung adenocarcinoma. *J Thorac Oncol* 2011; **6**: 244–85.
18 Noguchi M, Morikawa A, Kawasaki M *et al.* Small adenocarcinoma of the lung – histologic characteristics and prognosis. *Cancer* 1995; **75**: 2844–52.
19 Sobin LH, Gospodarowicz M, Wittekind C. *International Union Against Cancer: TNM Classification of Malignant Tumours*, 7th edn. West Sussex: Wiley-Blackwell, 2009; 136–46.
20 Katoh H, Ojima H, Kokubu A *et al.* Genetically distinct and clinically relevant classification of hepatocellular carcinoma: putative therapeutic targets. *Gastroenterology* 2007; **133**: 1475–86.
21 Soh J, Okumura N, Lockwood WW *et al.* Oncogene mutations, copy number gains and mutant allele specific imbalance (MASI) frequently occur together in tumor cells. *PLoS ONE* 2009; **4**: e7464.
22 He LR, Zhao HY, Li BK *et al.* Overexpression of eIF5A-2 is an adverse prognostic marker of survival in stage I non-small cell lung cancer patients. *Int J Cancer* 2011; **129**: 143–50.
23 Henken FE, Banerjee NS, Snijders PJ *et al.* PIK3CA-mediated PI3-kinase signalling is essential for HPV-induced transformation in vitro. *Mol Cancer* 2011; **10**: 71.
24 Ouellet V, Le Page C, Madore J *et al.* An apoptotic molecular network identified by microarray: on the TRAIL to new insights in epithelial ovarian cancer. *Cancer* 2007; **110**: 297–308.
25 Iyoda M, Kasamatsu A, Ishigami T *et al.* Epithelial cell transforming sequence 2 in human oral cancer. *PLoS ONE* 2010; **5**: e14082.
26 Justilien V, Fields AP. Ect2 links the PKCiota-Par6alpha complex to Rac1 activation and cellular transformation. *Oncogene* 2009; **28**: 3597–607.
27 Okayama H, Kohno T, Ishii Y *et al.* Identification of genes upregulated in ALK-positive and EGFR/KRAS/ALK-negative lung adenocarcinomas. *Cancer Res* 2012; **72**: 100–11.
28 Vazquez-Mena O, Medina-Martinez I, Juárez-Torres E *et al.* Amplified genes may be overexpressed, unchanged, or downregulated in cervical cancer cell lines. *PLoS ONE* 2012; **7**: e32667.
29 Cai C, Rajaram M, Zhou X *et al.* Activation of multiple cancer pathways and tumor maintenance function of the 3q amplified oncogene FNDC3B. *Cell Cycle* 2012; **11**: 1773–81.
30 Lake SL, Kalirai H, Dopierala J, Damato BE, Coupland SE. Comparison of formalin-fixed and snap-frozen samples analyzed by multiplex ligation-dependent probe amplification for prognostic testing in uveal melanoma. *Invest Ophthalmol Vis Sci* 2012; **53**: 2647–52.
31 Brunelli M, Bria E, Nottegar A *et al.* True 3q chromosomal amplification in squamous cell lung carcinoma by FISH and aCGH molecular analysis: impact on targeted drugs. *PLoS ONE* 2012; **7**: e49689.
32 Rácz A, Brass N, Heckel D, Pahl S, Remberger K, Meese E. Expression analysis of genes at 3q26–q27 involved in frequent amplification in squamous cell lung carcinoma. *Eur J Cancer* 1999; **35**: 641–6.
33 Yokoi S, Yasui K, Iizasa T, Imoto I, Fujisawa T, Inazawa J. TERC identified as a probable target within the 3q26 amplicon that is detected frequently in non-small cell lung cancers. *Clin Cancer Res* 2003; **9**: 4705–13.
34 Jenkins ZA, Hååg PG, Johansson HE. Human eIF5A2 on chromosome 3q25-q27 is a phylogenetically conserved vertebrate variant of eukaryotic translation initiation factor 5A with tissue-specific expression. *Genomics* 2001; **71**: 101–9.
35 Pelosi G, Del Curto B, Trubia M *et al.* 3q26 Amplification and polysomy of chromosome 3 in squamous cell lesions of the lung: a fluorescence in situ hybridization study. *Clin Cancer Res* 2007; **13**: 1995–2004.
36 Wiley SR, Schooley K, Smolak PJ *et al.* Identification and characterization of a new member of the TNF family that induces apoptosis. *Immunity* 1995; **3**: 673–82.
37 Hirata D, Yamabuki T, Miki D *et al.* Involvement of epithelial cell transforming sequence-2 oncoantigen in lung and esophageal cancer progression. *Clin Cancer Res* 2009; **15**: 256–66.
38 Miki T, Smith CL, Long JE, Eva A, Fleming TP. Oncogene ect2 is related to regulators of small GTP-binding proteins. *Nature* 1993; **362**: 462–5.
39 Fields AP, Justilien V. The guanine nucleotide exchange factor (GEF) Ect2 is an oncogene in human cancer. *Adv Enzyme Regul* 2010; **50**: 190–200.

40 Tatsumoto T, Xie X, Blumenthal R, Okamoto I, Miki T. Human ECT2 is an exchange factor for Rho GTPases, phosphorylated in G2/M phases, and involved in cytokinesis. *J Cell Biol* 1999; **147**: 921–8.
41 Yatabe Y, Kosaka T, Takahashi T, Mitsudomi T. EGFR mutation is specific for terminal respiratory unit type adenocarcinoma. *Am J Surg Pathol* 2005; **29**: 633–9.
42 Sugano M, Nagasaka T, Sasaki E *et al.* HNF4α as a marker for invasive mucinous adenocarcinoma of the lung. *Am J Surg Pathol* 2013; **37**: 211–8.
43 Murray NR, Kalari KR, Fields AP. Protein kinase Cι expression and oncogenic signaling mechanisms in cancer. *J Cell Physiol* 2011; **226**: 879–87.

Supporting Information

Additional supporting information may be found in the online version of this article:

Fig. S1. Array-comparative genomic hybridization analysis by Cancer Array-800 (3q region).

Fig. S2. Kaplan–Meier curves revealed difference between high and low ECT2 score.

Fig. S3. GeneChip Human Mapping 10K SNP array in 64 cases of small-sized lung adenocarcinoma.